Microbiology:

Catabolite Control Protein E (CcpE) Is a LysR-type Transcriptional Regulator of Tricarboxylic Acid Cycle Activity in *Staphylococcus aureus*

Torsten Hartmann, Bo Zhang, Grégory Baronian, Bettina Schulthess, Dagmar Homerova, Stephanie Grubmüller, Erika Kutzner, Rosmarie Gaupp, Ralph Bertram, Robert Powers, Wolfgang Eisenreich, Jan Kormanec, Mathias Herrmann, Virginie Molle, Greg A. Somerville and Markus Bischoff

J. Biol. Chem. 2013, 288:36116-36128.
doi: 10.1074/jbc.M113.516302 originally published online November 5, 2013

THE JOURNAL OF BIOLOGICAL CHEMISTRY VOL. 288, NO. 50, pp. 36116–36128, December 13, 2013

Catabolite Control Protein E (CcpE) Is a LysR-type Transcriptional Regulator of Tricarboxylic Acid Cycle Activity in *Staphylococcus aureus*[*]

Received for publication, September 5, 2013, and in revised form, October 15, 2013 Published, JBC Papers in Press, November 5, 2013, DOI 10.1074/jbc.M113.516302

Torsten Hartmann[‡], Bo Zhang[§], Grégory Baronian[¶1], Bettina Schulthess[‖2], Dagmar Homerova[3], Stephanie Grubmüller[‡‡], Erika Kutzner[‡‡], Rosmarie Gaupp[§§], Ralph Bertram[¶¶4], Robert Powers[§], Wolfgang Eisenreich[‡‡5], Jan Kormanec[**3], Mathias Herrmann[‡], Virginie Molle[¶1], Greg A. Somerville[§§6], and Markus Bischoff[‡6,7]**

From the [‡]Institute of Medical Microbiology and Hygiene, University of Saarland Hospital, 66421 Homburg/Saar, Germany, the [§]Department of Chemistry and the [§§]School of Veterinary Medicine and Biomedical Sciences, University of Nebraska, Lincoln, Nebraska 68583-0903, the [¶]Laboratoire de Dynamique des Interactions Membranaires Normales et Pathologiques, Université Montpellier 2, CNRS, UMR 5235, 34090 Montpellier, France, the [‖]Institute of Medical Microbiology, University of Zürich, 8006 Zürich, Switzerland, the [**]Institute of Molecular Biology, Slovak Academy of Sciences, 845 51 Bratislava, Slovak Republic, the [‡‡]Department of Biochemistry, Technische Universität München, 85748 Garching, Germany, and the [¶¶]Department of Microbial Genetics, University of Tübingen, 72076 Tübingen, Germany

Background: The TCA cycle is a central metabolic pathway that facilitates the adaption of bacteria to a nutrient-limited environment.
Results: Inactivation of CcpE in *Staphylococcus aureus* resulted in a decreased transcription of the aconitase encoding gene *citB*, and reduced TCA cycle activity.
Conclusion: CcpE affects the TCA cycle via direct transcriptional control of *citB*.
Significance: This is the first positive regulator of TCA cycle activity identified in this pathogen.

The tricarboxylic acid cycle (TCA cycle) is a central metabolic pathway that provides energy, reducing potential, and biosynthetic intermediates. In *Staphylococcus aureus*, TCA cycle activity is controlled by several regulators (*e.g.* CcpA, CodY, and RpiRc) in response to the availability of sugars, amino acids, and environmental stress. Developing a bioinformatic search for additional carbon catabolite-responsive regulators in *S. aureus*, we identified a LysR-type regulator, catabolite control protein E (CcpE), with homology to the *Bacillus subtilis* CcpC regulator. Inactivation of *ccpE* in *S. aureus* strain Newman revealed that CcpE is a positive transcriptional effector of the first two enzymes of the TCA cycle, aconitase (*citB*) and to a lesser extent citrate synthase (*citZ*). Consistent with the transcriptional data, aconitase activity dramatically decreased in the *ccpE* mutant relative to the wild-type strain. The effect of *ccpE* inactivation on *citB* transcription and the lesser effect on *citZ* transcription were also reflected in electrophoretic mobility shift assays where CcpE bound to the *citB* promoter but not the *citZ* promoter. Metabolomic studies showed that inactivation of *ccpE* resulted in increased intracellular concentrations of acetate, citrate, lactate, and alanine, consistent with a redirection of carbon away from the TCA cycle. Taken together, our data suggest that CcpE is a major direct positive regulator of the TCA cycle gene *citB*.

Carbon catabolite repression (CCR)[8] in bacteria is a widespread, regulatory phenomenon that represses transcription of genes and operons involved in the catabolism of non-preferred carbon sources when the preferred carbon source(s) are present. CCR has been studied extensively in *Bacillus subtilis* and serves as the prototype of CCR-regulated gene expression in Gram-positive bacteria (reviewed in Refs. 1 and 2). In *B. subtilis*, the catabolite control protein A (CcpA) acts in concert with the small phosphocarrier proteins histidine-containing protein (HPr) and catabolite repression HPr (Crh) to regulate transcription in response to carbohydrate availability. In addition, the metabolite-activated bifunctional HPr kinase/phosphorylase is involved in CCR through its action of phosphorylating and dephosphorylating HPr (3, 4). There are several other proteins in *B. subtilis* that contribute to CCR either in cooperation with, or independently of CcpA, including CcpC (5, 6), CcpN (7), CitR (8), Crh (9), CodY (10), and GlcU (11) (reviewed in Ref. 1). In *Staphylococcus aureus*, homologs of CcpA and CodY regulate the transcription of numerous metabolic and biosynthetic genes and virulence determinants; thereby, linking staphylococcal carbon metabolism with pathogenicity (reviewed in Ref. 12).

To identify additional CCR elements in *S. aureus*, we compared the genomes of *S. aureus* strain Newman with that of *B.*

* This work was supported, in whole or in part, by National Institutes of Health Grant AI087668 (to G. A. S. and R. P.) and Grants BI 1350/1-1 and BI 1350/1-2 from the Deutsche Forschungsgemeinschaft (DFG).
[1] Supported by the region Languedoc-Roussillon-Chercheur d'Avenir grant.
[2] Supported by Swiss National Science Foundation Grant 31-117707.
[3] Supported by Grant 2/0028/12 from the Slovak Academy of Sciences.
[4] Supported by DFG Grants BE 4038/1 and BE 4038/2.
[5] Supported by the DFG Grants EI-384/5-1 and EI-384/5-2.
[6] Both authors contributed equally to this work.
[7] To whom correspondence should be addressed. Tel.: 49-6841-162-39-63; Fax: 49-6841-162-39-85; E-mail: markus.bischoff@uniklinikum-saarland.de.

[8] The abbreviations used are: CCR, carbon catabolite repression; TCA, tricarboxylic acid; PCA, principal component analysis; HSQC, heteronuclear single quantum coherence; qRT-PCR, real-time reverse transcription PCR.

TABLE 1
Strains and plasmids used in this study

Strain or plasmid	Relevant genotype or characteristic(s)[a]	Reference or source
S. aureus		
RN4220	NCTC 8325-4 r^- m^+ (restriction-negative, modification-positive)	(55)
Newman	Clinical isolate (ATCC 25904); CP-5 producer	(56)
THa	RN4220 Δ*ccpE::lox66-aphAIII-lox71*, Kan^r	This study
TH01	Newman Δ*ccpE::lox72*	This study
TH01c	TH01 harboring plasmid pTH2c cis-integrated at the NWMN_0640 locus, leading to a duplication of the NWMN_0640 gene, *ccpE*$^+$, Tc^r	This study
B. subtilis		
AF21	Δ*amyE::*Φ(*citBp21-lacZ cat*), Cm^r	(57)
CJB9	Δ*amyE::*Φ(*citBp21-lacZ cat*) *ccpC::spc*, Cm^r, Spc^r	(6)
E. coli		
DH5α	*hsdR*17(r_k^- m_k^+) *deoR endA1 gyrA96 recA1 relA1 supE44 thi*-1 F^- λ$^-$ Δ(*lacZYA-argF*) U169 φ80 *lacZ*ΔM15	Invitrogen
SCS110	*dam dcm rpsL* (Str^r) *thr leu endA thi-1 lacY galK galT ara tonA tsx supE*44 Δ(*lac-proAB*) [*F′ traD36 proAB lacI*^{q}ZΔM15]	Stratagene
Plasmids		
pBT	1.6-kb PCR fragment of the *tet*(L) gene of pHY300PLK into AlwI26I-digested pBC SK(+) (Stratagene); Tc^r	(58)
pBT2-arcA	Allelic replacement vector for *S. aureus arcA*, harboring the *lox66-aphAIII-lox71* cassette; Kan^r	(13)
pBT *lox-aph*	pBT with a 1.6 kb *lox66-aphAIII-lox71* fragment obtained from pBT2-arcA cloned into the PstI site of pBT; Kan^r, Tc^r	This study
pBus1	*E. coli-S. aureus* shuttle plasmid with multicloning site from pBluescript II SK (Stratagene) and the *rrn*T14 terminator sequence from pLL2443; Tc^r	(14)
pRAB1	*cat, bla*, P_{pagA}-*cre*; pBT2 derivative; expression of Cre in staphylococci; Cm^r	(13)
pT7HMT	pET28-based expression vector, allowing a T7 polymerase-driven expression of hexahistidine-tagged fusion proteins, Kan^r	(59)
pT7HMT-ccpE	pT7HMT derivative harboring the *ccpE* ORF cloned into the SalI and NotI sites of the vector, Kan^r	This study
pTH2	pBT with a 3 kb fragment covering the *NWMN_0641* flanking regions and the *lox66-aphAIII-lox71* resistance cassette fully replacing the *ccpE* ORF, Tc^r	This study
pTH2c	pBT with a 2 kb fragment covering the *ccpE* ORF and 1 kb of the upstream region including the NWMN_0640 ORF, Tc^r	This study
pTH3	pBus1 with a 1.7-kb fragment covering the *B. subtilis ccpC* promoters P1/P2 and the *ccpC* ORF, Tc^r	This study
pTH4	pBus1 with a 1.7-kb fragment covering the *B. subtilis ccpC* promoters P1/P2 and the *ccpE* ORF, Tc^r	This study

[a] Abbreviations: Cm^r, chloramphenicol resistant; Kan^r, kanamycin resistant; Spc^r, spectinomycin resistant; Tc^r, tetracycline resistant; ORF, open reading frame.

TABLE 2
Primers used in this study

Primer		Sequence (5′- 3′)[a]
Construction primer		
MBH152	forward	GCAAATTGAGCTCTATCTTTAGAGC
MBH153	reverse	gtcgGATCCGAGCATGTTGCAATTGCC
MBH154	forward	gtcggtacCTGGCGTCGCCTAATTGATAGG
MBH155	reverse	gtcctcgaGTATGGCTGCAGCTTGAATTAC
MBH225	forward	gtcggatcCAGAATAGATTTGATGCTTCAGC
MBH226	reverse	gtcggtACCAACTACGTTCAATTTAACCG
MHB239	forward	ggggtcgacTATGAAGATTGAAGACTATCGTTTAC
MBH255	reverse	gtcggtaccTGATTTTCAATATCATATGTATCAC
MBH338	reverse	GCATGTCGaCCTCCTTTTTGTTATCAATAAG
MBH341	forward	ctgtctAGATCAACGATATAGAGACAGGG
5′-RACE primer		
5`RACE-Adapter (RNA)		GAUAUGCGCGAAUUCCUGUAGAACGAACACUAGAAGAAA
NWMN_0640-RT		TCTACTGTACACGCATTACC
citB-RT		ACGTCATCCATTGCTTTACG
RACE_PCR_5′		GATATGCGCGAATTCCTGTAGAACG
NWMN_0640-PCR		CGTGACTAAGCCTATAATACCC
citB-PCR		GTAATACCTTGCTCTTCTACAGC
Northern probe primer		
MBH279	forward	GGTATTATAGGCTTAGTCACG
MBH280	reverse	GCAGTACATGATTTTCTTTTGG
MBH281	forward	AGACGAAACGAAAACGTTACG
MBH282	reverse	GTAACTTTGTAACATCATCTCG
Real-time RT PCR primer		
Bs ccpC	forward	TGTGGAAAAGTATCCGAATGCA
Bs ccpC	reverse	CTGCTCCACCCGGTTATGA
ccpE	forward	CCGCTGATTCGTTCGACAT
ccpE	reverse	CAATTGCAACATGCTCGGAT
citB	forward	CAAGATCATCAAGTGCCTATTCGT
citB	reverse	CGTGATTACCACGTCTTGAACC
Bs citB	forward	TAATCGGCGCGAAACTTGTC
Bs citB	reverse	CAGTAGCTGTTGTTCCGTTTGG
citZ	forward	CCGTAGGTTCTCTGAAAGGGC
citZ	reverse	AACATCGTCATAACTTGTTCGTTTG
gyrB	forward	GACTGATGCCGATGTGGA
gyrB	reverse	AACGGTGGCTGTGCAATA
Bs gyrB	forward	CATTGGCGAAACGGATCATA
Bs gyrB	reverse	GGGTCCGGGACAAAATGTG
EMSA primer		
ccpE	forward	CAAATAAAGCCTAAGCAATAT
ccpE	reverse	AGTAAACGATAGTCTTCAATC
citBp	forward	ATCATTTCTGTCCCACTCCCATC
citBp	reverse	GTAAGTATAACTTTGGCCATTCAAGTC
citZp	forward	ATTGTAAAATTCATGGATTATTCAC
citZp	reverse	CTAAACCTCTTTGTAATTCTGCCAT
NWMN-0640p	forward	GTGATCAATGAAGTGGTTTGAAGG
NWMN-0640p	reverse	CTTTTACCTCTGTGTATTCCCTATC

[a] Small letters represent nucleotides that do not fit with the target sequence. Restriction sites used for cloning are underlined.

subtilis strain 168 and found that *S. aureus* had uncharacterized homologs of *B. subtilis* genes that are known to affect the regulation of carbon catabolism. Here we report the identification of a putative carbon catabolite responsive regulator, CcpE (NWMN_0641), that affects the central metabolism by regulating tricarboxylic acid (TCA) cycle activity via transcriptional control of the aconitase-encoding gene *citB*.

EXPERIMENTAL PROCEDURES

Bacterial Strains and Culture Conditions—The bacterial strains and plasmids used in this study are listed in Table 1. *S. aureus* strains were grown in Luria-Bertani Lennox (LB-L) medium (BD, Heidelberg, Germany) and *B. subtilis* strains were grown in TSS minimal medium supplemented with 0.2% (w/v) glutamine and 0.5% (w/v) glucose (6). All strains were grown at 37 °C and aerated at 230 rpm with a flask-to-medium volume ratio of 10:1. Antibiotics, when used, were added to the medium at the following concentrations (per milliliter): 10 μg of chloramphenicol, 50 μg of kanamycin, and 8 μg of tetracycline.

Construction of a S. aureus ΔccpE Mutant—1-Kilobase fragments, containing the flanking regions of the *ccpE* (NWMN_0641) gene were amplified by PCR from chromosomal DNA of *S. aureus* strain Newman using primer pairs MBH154/MBH155 and MBH152/MBH153, respectively (primer sequences are listed in Table 2). The PCR products were digested with KpnI/XhoI and BamHI/SacI, respectively, and cloned together with the XhoI/BamHI-digested *lox66-aphAIII-lox71* resistance cas-

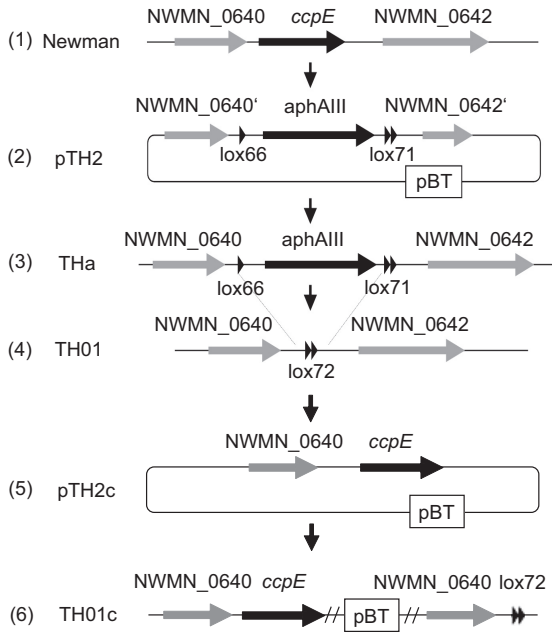

FIGURE 1. **Schematic representation of the *ccpE* region of *S. aureus* and the strategies used to obtain the Δ*ccpE* mutant TH01 and the *cis*-complemented derivative TH01c.** *1*) genetic organization of the *S. aureus* Newman *ccpE* region. Open reading frames (*arrowed boxes*) and promoters (*vertical arrows*) are indicated. *2*) a 3-kb fragment containing the *lox66-aphAIII-lox71* resistance cassette and the flanking regions of the *ccpE* gene was cloned into the vector pBT to generate plasmid pTH2. *3*) plasmid pTH2 was electroporated into *S. aureus* strain RN4220 to obtain THa (RN4220 Δ*ccpE*::*lox66-aphAIII-lox71*), which was used as a donor for transducing the *aphAIII*-tagged *ccpE* deletion into other *S. aureus* strains. *4*) a marker-free Δ*ccpE* mutant of *S. aureus* strain Newman was obtained by treating a Δ*ccpE*::*lox66-aphAIII-lox71* positive derivative of strain Newman with a Cre recombinase. *Dotted lines* between *3* and *4* indicate the region removed by Cre. *5*) a 2-kb fragment covering the *ccpE* ORF and 1 kb of the upstream region including the NWMN_0640 ORF was cloned into the vector pBT to generate plasmid pTH2c. *6*) a *dam*- and *dcm*-methylation free aliquot of plasmid pTH2c was directly electroporated into TH01 to obtain Th01c.

sette (obtained from pBT2-arcA) into suicide vector pBT to generate plasmid pTH2 (Fig. 1). Plasmid pTH2 was electroporated into *S. aureus* strain RN4220 to obtain strain THa, in which the *ccpE* gene was replaced by the *lox66-aphAIII-lox71* cassette by allelic replacement. THa was then used as a donor for transducing the *ccpE* deletion into other *S. aureus* strains. The marker-free Δ*ccpE* mutant TH01 of *S. aureus* strain Newman was constructed by treatment with the Cre recombinase expressed from the temperature-sensitive vector pRAB1 (13), which was subsequently removed from TH01 by culturing the strain at 42 °C. The deletion of *ccpE* in TH01 was confirmed by PCR, pulsed-field gel electrophoresis of total genome SmaI digests, and DNA sequencing.

Construction of the S. aureus ccpE cis-complementation Strain TH01c—For *cis*-complementation of the *ccpE* mutation in strain TH01, a 2-kb fragment containing the wild-type *ccpE* allele and 1 kb of the upstream region including the NWMN_0640 open reading frame, was amplified by PCR from chromosomal DNA of *S. aureus* strain Newman using the primer pair MBH225/MBH226. The resulting PCR product was digested with BamHI/KpnI, and subsequently cloned into BamHI/KpnI-digested vector pBT to generate the suicide plasmid pTH2c (Fig. 1). The plasmid was transformed into and purified out of *dam*- and *dcm*-negative *Escherichia coli* strain SCS110 (Stratagene), and electroporated into *S. aureus* strain TH01 to obtain the *cis*-complementation strain TH01c (TH01Δ*ccpE*::*pTH2c*). Restoration of the *ccpE* wild-type gene was verified by sequencing of the respective DNA fragment.

Construction of the B. subtilis ccpC Promoter-B. subtilis ccpC and B. subtilis ccpC promoter-ccpE Trans-complementation Plasmids—Nucleotide sequences covering the *B. subtilis ccpC* promoter and gene were amplified by PCR from *B. subtilis* strain AF21 using the primer pairs MBH341/MBH255 and cloned into XbaI/KpnI-digested shuttle vector pBus1 (14). Similarly, the *ccpE* gene from *S. aureus* strain Newman was amplified by PCR using primers MBH239/MBH226 and the *ccpE* fragment was digested with SalI/KpnI and cloned into pBus1 that was digested with the same restriction enzymes. *ccpC* promoters P1 and P2 were amplified by PCR using primer pair MBH341/MBH338 and *B. subtilis* strain AF21 DNA. The PCR product was digested with XbaI/SalI and cloned into pre-digested pBus1 harboring the *S. aureus ccpE* open reading frame. The resulting plasmids, pTH3 (*Bs ccpC* P1/2-*ccpC*) and pTH4 (*Bs ccpC* P1/2-*Sa ccpE* fusion), were used to transform competent cells of CJB9 or to electroporate RN4220. The resulting derivatives of RN4220 were then used as a donor for transducing it into *S. aureus* strain TH01.

Measurement of Glucose, Acetate, and Ammonia Concentrations in Culture Supernatants—Bacteria were cultivated in LB-L supplemented with 0.1% glucose, and aliquots of the cultures (2 ml) were removed hourly over a period of 12 h, centrifuged for 5 min at 15,000 × *g* at 4 °C, and the culture supernatants stored at −20 °C until use. Glucose, acetate, and ammonia concentrations were determined with kits from R-Biopharm (Darmstadt, Germany) according to the manufacturer's directions.

Aconitase and Citrate Synthase Activity Assays—Bacteria were cultivated in LB-L as described before, and aliquots of the cultures (2 ml) were removed after 3, 6, 9, and 12 h of growth. Cells were harvested by centrifugation for 5 min at 15,000 × *g* and 4 °C, cell pellets were resuspended in 850 μl of lysis buffer (90 mM Tris, pH 8.0, and 100 μM fluorocitrate), and bacteria were mechanically disrupted in a Fast Prep instrument (Qbiogene, Heidelberg, Germany) at a speed of 6.0 for 30 s. Lysates were centrifuged for 1 min at 15,000 × *g* and 4 °C, and total protein concentrations of the supernatants were determined according to the method described by Bradford (17). Aconitase activities were assayed in cell-free supernatants as described previously (15). One unit of aconitase activity was defined as the amount of enzyme necessary for a ΔA_{240} min^{-1} of 0.0033 (16). Citrate synthase activities were determined with the Citrate Synthase Assay Kit (Sigma) according to the manufacturer's recommendations, with the following modifications. Cell pellets were suspended in CelLytic M Cell Lysis Reagent, and cell-free supernatants were obtained as described above. 10-μl aliquots of the cell-free lysate were mixed at room temperature with 0.1 mM 5,5′-dithiobis-(2-nitrobenzoic acid) and 0.3 mM acetyl coenzyme A (CoA) in 1× assay buffer (Sigma). The solutions were mixed gently, and the absorbance of the reaction mixtures at 412 nm (A_{412}) were followed for 1.5 min to obtain a background reading. After the addition of 0.5 mM oxaloacetate, the absorbance of the reaction mixtures at A_{412} were monitored for an additional 1.5 min to detect the formation of 5-thio-2-nitrobenzoic acid. Citrate syn-

thase activity units were calculated as micromoles of 5-thio-2-nitrobenzoic acid produced (*i.e.* CoA-SH released) per minute per milligram of total protein (μmol/min/mg).

Determination of Citrate by GC/MS—Lyophilized cell pellets (10 mg dry weight) of Newman, TH01, and TH01c (each harvested after 8 h of growth in LB-L) were combined with 0.5-ml glass beads (Roth, Karslruhe, Germany; 0.25–0.5 mm diameter) and 1 ml of methanol was added. This mixture was subjected to homogenizer lysis (FastPrep FP120, QBiogene; 3 cycles each of 20 s at 6.5 m/s). After cell disruption, the cell debris and glass beads were separated by centrifugation (10 min at 5,000 × *g*). The supernatant (0.5 ml) was dried under a stream of nitrogen. The residue was dissolved in 50 μl of methoxyamine hydrochloride (solution of 20 mg/ml of pyridine) and reacted at 30 °C for 90 min. 50 μl of *N*-methyl-*N*-(trimethylsilyl)trifluoroacetamide with 1% trimethylchlorosilane (Fluka, Germany) were added and the mixture was incubated at 37 °C for 30 min. GC/MS analyses were performed on a GC/MS Shimadzu QP 2010 Plus (Shimadzu, Duisburg, Germany) equipped with a fused silica capillary column (Equity TM-5; 30 m × 0.25 mm, 0.25-μm film thickness; SUPELCO, Bellafonte, PA) and a QP-5000 mass selective detector (Shimadzu, Duisburg, Germany) working with electron impact ionization at 70 eV. An aliquot (1 μl) of the solution was injected in a 1:10 split mode at an interface temperature of 250 °C and a helium inlet pressure of 76 kilopascal. The column was developed at 70 °C for 5 min and then with a temperature gradient of 5 °C/min to a final temperature of 310 °C that was held for 1 min. Data were collected using the LabSolutions software (Shimadzu, Duisburg, Germany). Compound peaks were assigned by comparison of the resulting mass spectra with those of a spectral library (NIST05, Shimadzu) and with data of injected reference samples under the same conditions.

Transcriptional Analyses—For Northern blot experiments, overnight cultures of *S. aureus* were diluted to an A_{600} of 0.05 into fresh pre-warmed LB-L and grown at 37 °C and 230 rpm. Samples were removed from the culture at the indicated times and centrifuged at 9,000 × *g* and 4 °C for 2 min, the culture supernatants were discarded, and the cell pellets were snap frozen in liquid nitrogen. Total RNAs were isolated according to Ref. 18, and blotting, hybridization, and labeling were performed as described previously (19). Primer pairs MBH279/MBH280 and MBH281/MBH282 were used to generate digoxigenin-labeled NWMN_0640- and *ccpE*-specific probes by PCR labeling, respectively.

For the quantification of transcripts by real-time reverse transcription-PCR (qRT-PCR), RNA isolations and qRT-PCRs were carried out essentially as described in Ref. 20. The obtained cDNA was used for real-time amplification with specific primers (Table 2) and 20 ng of cDNA/reaction. mRNA levels were normalized against the mRNA level of *gyrB*, which is constitutively expressed under the conditions analyzed (21). The amounts of different transcripts were expressed as the *n*-fold difference relative to the control gene ($2^{-\Delta CT}$, where ΔC_T represents the difference in threshold cycle between the target and control genes).

Determination of Transcriptional Start Sites of NMMN_0640 and citB—Strain Newman was grown for 3 h as described and the bacteria were harvested by centrifugation at 8,000 × *g* for 10 min. RNA isolation was carried out as described above. The transcriptional start points of *NMMN_0640* and *citB* were determined by rapid amplification of cDNA ends essentially as described by Ref. 22. The reverse transcription of 8.2 μl of the ligated RNA was carried out with *NMWN_0640* or *citB*-specific primers (Table 2) with the High Capacity cDNA Reverse Transcription Kit (Invitrogen) according to the manufacturer's instructions. 2 μl of the cDNA was amplified by PCR using a primer complementary to the RNA adapter sequence, and a specific primer for *NMWN_0640* or *citB* (Table 2) closer to the 5′-end than the primers used for the reverse transcription. Finally, the PCR products were sequenced.

Antibody Production and Immunoblotting—Polyclonal anti-CcpE antibodies were raised by injecting 500 μg of the His-tagged recombinant CcpE into rabbits (Eurogentec, Liege, Belgium). The resulting crude antisera were purified against the immobilized CcpE antigen. For the determination of CcpE, cytoplasmic protein extracts were isolated from *S. aureus* cell cultures grown for 3, 6, 9, and 12 h in LB-L at 37 °C as described previously (23), and protein fractions (20 μg/lane) were separated using SDS-PAGE, blotted onto a nitrocellulose membrane, and subjected to Western blot analysis using the antigen-purified polyclonal anti-CcpE antiserum.

Electrophoretic Mobility Shift Assays—The DNA probes for electrophoretic mobility shift assays (EMSAs) were generated by PCR using *S. aureus* strain Newman chromosomal DNA as a template, and primer pairs (listed in Table 2) that amplified the DNA regions preceding the *ccpE*, *citB*, *citZ*, and NWMN_0640 ORFs. The 5′-ends of the double-stranded PCR products were labeled using [γ-^{32}P]ATP and T4 polynucleotide kinase. A typical assay mixture contained (in 20 μl) 10 mM Tris-HCl, pH 7.5, 50 mM NaCl, 1 mM EDTA, 1 mM DTT, 0.1 μg of nonspecific competitor (poly(dI-dC)), 5% (v/v) glycerol, radioactive DNA probe (2000 cpm ml^{-1}), and various amounts (0, 15, 65, 130, and 200 nM) of purified CcpE. After 30 min of incubation at room temperature, 20 μl of this mixture was loaded into a native 4% (w/v) polyacrylamide Tris borate-EDTA Ready Gel (Bio-Rad) and electrophoresed in 1% Tris borate-EDTA (v/v) buffer for 1 h at 100 V cm^{-1}. Radioactive species were detected by autoradiography using direct exposure to films.

NMR Sample Preparation—*S. aureus* strains were grown in LB-L supplemented with 0.1% glucose as described above. For two-dimensional ^{1}H,^{13}C-HSQC analysis LB-L medium containing 0.1% [$^{13}C_6$]glucose (Cambridge Isotope Laboratories) was used for the main cultures. NMR samples for intracellular metabolite analysis were prepared from independent cultures in exponential (3 h) and post-exponential (8 h) growth phase. The extraction of the metabolome from cell lysates followed our previously published protocols (24, 25).

NMR Data Collection, Analysis, and Interpretation—Followed as previously published (24, 25). Briefly, NMR spectra were collected at 293 K on a Bruker 500 MHz DRX Avance spectrometer equipped with a triple-resonance, *Z*-axis gradient 5-mm TXI cryoprobe, a BACS-120 sample changer, automatic tune and match, and Icon NMR for automated data collection.

The two-dimensional time 0 extrapolated $^{1}H,^{13}C$-HSQC ($HSQC_0$) NMR spectra were collected as described by Hu and colleagues (26) to measure absolute metabolite concentrations and concentration changes. A set of three $HSQC_0$ spectra were collected for the six replicates for a total of 18 two-dimensional $^{1}H,^{13}C$-HSQC spectra per class. One-dimensional ^{1}H NMR spectra were processed in the ACD/one-dimensional NMR manager version 12.0 (Advanced Chemistry Development, Inc.) and the two-dimensional $^{1}H,^{13}C$-HSQC spectra were processed using the NMRPipe software package (27). Peak peaking and peak matching were performed using NMRViewJ version 8.0 (28). The metabolite assignments relied on the Human Metabolomics Database (HMDB), Madison Metabolomics Consortium Database (MMCD), and Biological Magnetic Resonance Data Bank (BMRB) (29–31). Metabolite concentration changes between strains TH01 and Newman were calculated relative to strain Newman using the following formula: $\delta = ([TH01] - [\text{Newman}])/\max([TH01],[\text{Newman}])$. These relative concentration changes for each of the six replicates were plotted as an Enhanced Heat Map using *R* with a gplots package and using a color-scale from −1 to 1. Metabolic network map was generated using the Cytoscape software package (32, 33) and verified based on consistency with the KEGG (34) and MetaCyc (35) databases.

50 or 500 μM 3-(trimethylsilyl)propionic acid-2,2,3,3-d_4 sodium salt were used as an internal standard for the one-dimensional ^{1}H and two-dimensional $^{1}H,^{13}C$-HSQC NMR experiments, respectively. 3-(Trimethylsilyl)propionic acid-2,2,3,3-d_4 was used for chemical shift referencing and for normalization of the NMR spectra.

The 10 replicates from each class were randomly interleaved during the one-dimensional ^{1}H NMR data collection, where the spectra were collected using excitation sculpting (36) to efficiently remove the solvent and maintain a flat baseline, eliminating any need for baseline collection that may induce artifacts in the multivariate statistical analysis. After Fourier transformation and phase correction, residual water, and buffer peaks were removed from the spectra, the entire one-dimensional ^{1}H NMR spectra were normalized using center averaging and binned using intelligent bucketing. Noise regions were eliminated and then the bins were scaled using center averaging prior to principal component analysis (PCA) and orthogonal projection to latent structures discriminate analysis (37).

Statistical Analyses—SIMCA12.0+ (UMETRICS) was used for PCA, orthogonal projection to latent structures discriminate analysis, and generating S-plots and loadings plots. Our PCA/projection to latent structures discriminate analysis utilities were used for statistical analysis of group separation in the PCA and orthogonal projection to latent structures discriminate analysis scores plots (38, 39). Statistical significances for other results were assessed using Student's *t* test or Mann-Whitney *U* test. *p* values <0.05 were considered significant.

RESULTS

Identification of Potential Carbon Metabolism Affecting Factors in S. aureus Strain Newman—A bioinformatic comparison of the genomes of *B. subtilis* isolate 168 (GenBank™ number AL009126.3) and *S. aureus* strain Newman (accession number AP009351.1) suggested that the strain Newman genome might have genes whose products have been associated with CCR in *B. subtilis* (reviewed in Ref. 1). One uncharacterized gene was NWMN_0641 (renamed here as *ccpE*), which shared 61% similarity and 35% identity to the *B. subtilis* citrate-responsive regulator CcpC, and like CcpC it was predicted to encode for a putative transcriptional regulator of the LysR family. These observations and the fact that CcpC is a regulator of TCA cycle genes *citZ* (encoding citrate synthase) and *citB* (encoding aconitase) (6), led us to examine the function of CcpE in *S. aureus*.

Transcriptional Organization of the ccpE Locus in S. aureus Strain Newman—Our microarray analysis of σ^B-mediated transcriptional changes (40) suggested that *ccpE* might form a bicistronic operon with the open reading frame (ORF) NWMN_0640. Further bioinformatic analysis of this region suggested that both genes were likely controlled by a promoter located upstream of NWMN_0640. To test this suggestion, we assessed the transcription of NWMN_0640 and *ccpE* by Northern blotting (Fig. 2*A*). This Northern blot analysis revealed *ccpE*-specific transcripts with sizes of ~4.1, 2.9, 2.3, and 1.5 kb. The 2.9- and 1.5-kb transcripts migrated on the gel to the same extent as the 16 S and 23 S rRNAs; hence, they might represent degradation products of higher molecular weight transcripts. That being said, all transcripts were detectable throughout the growth cycle and the transcription profiles of *ccpE* and NWMN_0640 were nearly identical. Based on these results, and on the genetic organization of the *ccpE* locus (Fig. 2*B*), we hypothesized that all transcripts originate from a single promoter in front of NWMN_0640, which would give rise to a NWMN_0640/*ccpE*-encoding 2.3-kb transcript, and a larger NWMN_0640/*ccpE*/NWMN_0642/3-encoding 4.1-kb transcript.

To identify the transcriptional start point of NWMN_0640, we performed a 5′-RACE experiment that identified a transcriptional start point 14 bp upstream of the proposed start point of the NWMN_0640 ORF, and immediately upstream of the putative ribosomal binding site of this ORF (Fig. 2*C*). The transcriptional start point is preceded by nucleotide sequence ATGACA-17-TATAAT that strongly matched with the −35 and −10 hexamers identified in the promoters of genes shown to be transcribed by *S. aureus* σ^A containing RNA polymerase (41, 42).

Because many LysR-type of regulators display autocrine regulation of their own transcription (43), we determined the capacity of CcpE to bind to its own promoter. To do this, purified CcpE was used in electrophoretic mobility shift assays with a PCR probe covering the genomic region preceding the NWMN_0640 ORF (Fig. 2*D*). As expected, a clear, dose-dependent shift with CcpE and the radioactively labeled NWMN_0640 promoter probe fragment was observed, suggesting that CcpE affects its own transcription. This DNA binding activity was specific, as an EMSA using a DNA probe covering the region preceding the *ccpE* ORF did not cause a mobility shift. Taken together, our data suggest that *ccpE* is transcribed in a bicistronic message using a promoter upstream of *NWMN_0640*, and that this promoter is subjected to autocrine regulation by CcpE.

Inactivation of ccpE in S. aureus Strain Newman—Using the *cre-lox*-based deletion system described for *staphylococci* by Leibig and colleagues (13), we created a marker-less deletion of *ccpE* in *S. aureus* strain Newman, giving rise to strain TH01. In

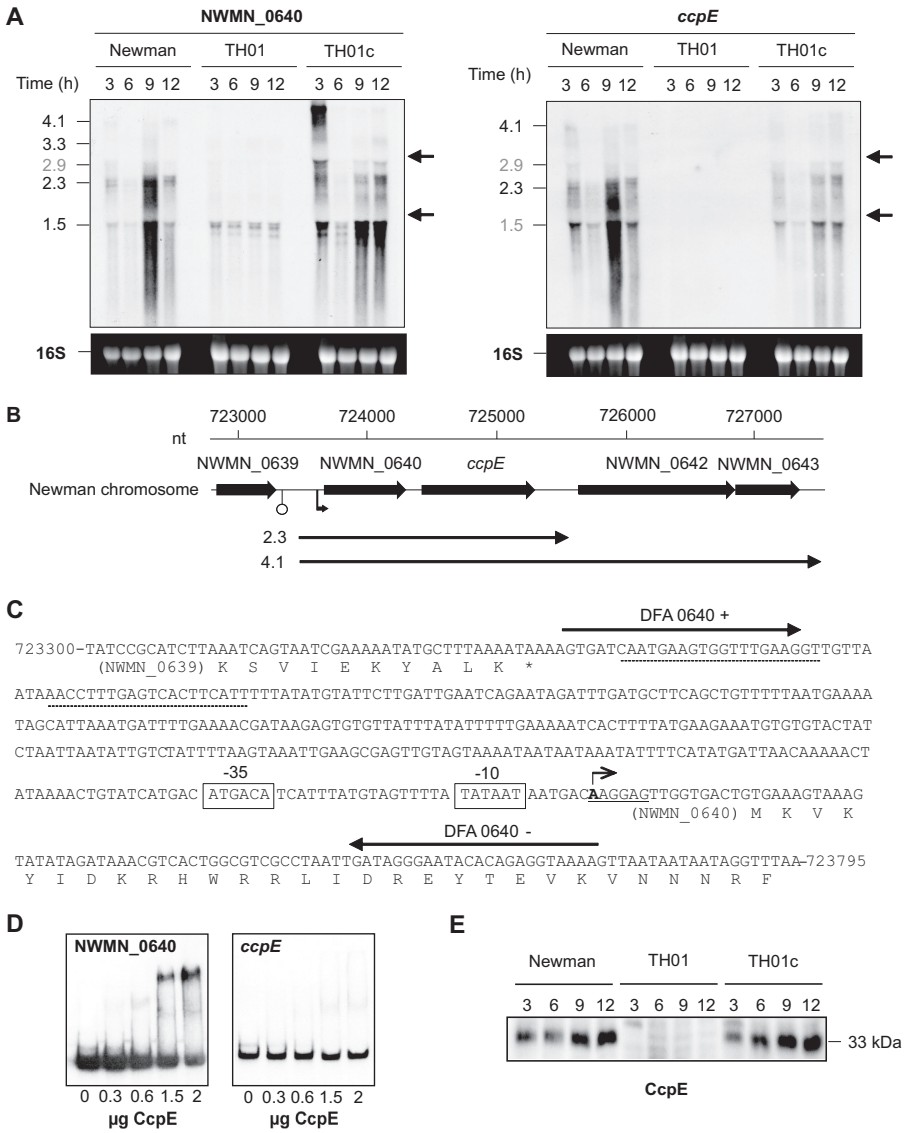

FIGURE 2. **Transcriptional organization of the *ccpE* locus of *S. aureus* Newman.** *A*, Northern blot of NWMN_0640 and *ccpE* transcriptions in strains Newman, TH01 (Δ*ccpE*), and the complemented TH01c during growth in LB-L. Approximate transcript sizes are indicated on the *left*. Ethidium bromide-stained 16 S rRNA are presented to indicate equivalent RNA loading. *B*, schematic representation of the *ccpE* region of *S. aureus*. Proposed ORFs, promoters, terminators, and transcripts identified by Northern analyses are indicated. ORF notations and nucleotide (*nt*) numbers correspond to those of the respective genomic regions of strain Newman (GenBank accession number AP009351.1). *C*, nucleotide sequence of the region preceding the NWMN_0640 open reading frame. The transcriptional start point identified by RACE (*bent arrow*), putative −35 and −10 boxes (*boxes*), terminator sequences (*hatched lines*), and primers used to amplify the NWMN_0640-*ccpE* promoter fragment used in EMSA (*horizontal arrows*) are indicated. *D*, binding activity of CcpE to the DNA regions preceding the NWMN_0640 and *ccpE* ORFs. The PCR-amplified DNA fragments were radioactively labeled and incubated with the amount of purified CcpE indicated. The results are representative of at least two independent experiments. *E*, Western blot analysis of CcpE in cytosolic extracts of strains Newman, TH01, and TH01c cells grown in LB-L to the time points indicated. The results are representative of at least two independent experiments.

addition, a *cis*-complemented derivative was created by integrating the NWMN_0640/*ccpE* containing suicide plasmid, pTH2c, into the deletion site of strain TH01, resulting in strain TH01c (Fig. 1). Sequencing of the respective genome regions confirmed that the mutations occurred as expected. Furthermore, Northern blot analysis qualitatively confirmed that strain TH01 did not produce a *ccpE*-specific transcript, whereas strain TH01c expressed *ccpE* at a level comparable with that of the wild-type strain (Fig. 2*A*). Probing total RNA from TH01 and TH01c with a NWMN_0640-specific probe also confirmed the deletion of *ccpE* in TH01, as we detected in strain TH01 NWMN_0640-specific transcripts of ~3.3 and 1.5 kb. These mRNA sizes are consistent with the deletion of 800 bp of the *ccpE* locus in this mutant. Importantly, complementation restored all NWMN_0640-specific transcripts found in the wild-type strain and also transcripts that were identified in TH01. This latter result was expected due to our complementation strategy that created a duplication of the NWMN_0640 gene due to the insertion of the suicide plasmid pTH2c into the NWMN_0640 ORF (Fig. 1). Taken together, these data confirmed that the correct gene was inactivated and that wild-type transcription profiles could be restored by complementation.

To assess the production of CcpE in *S. aureus*, rabbit polyclonal antibodies were generated against CcpE and used in Western blot analyses of cytosolic protein fractions from strains Newman, TH01, and TH01c grown in LB-L (Fig. 2*E*). In

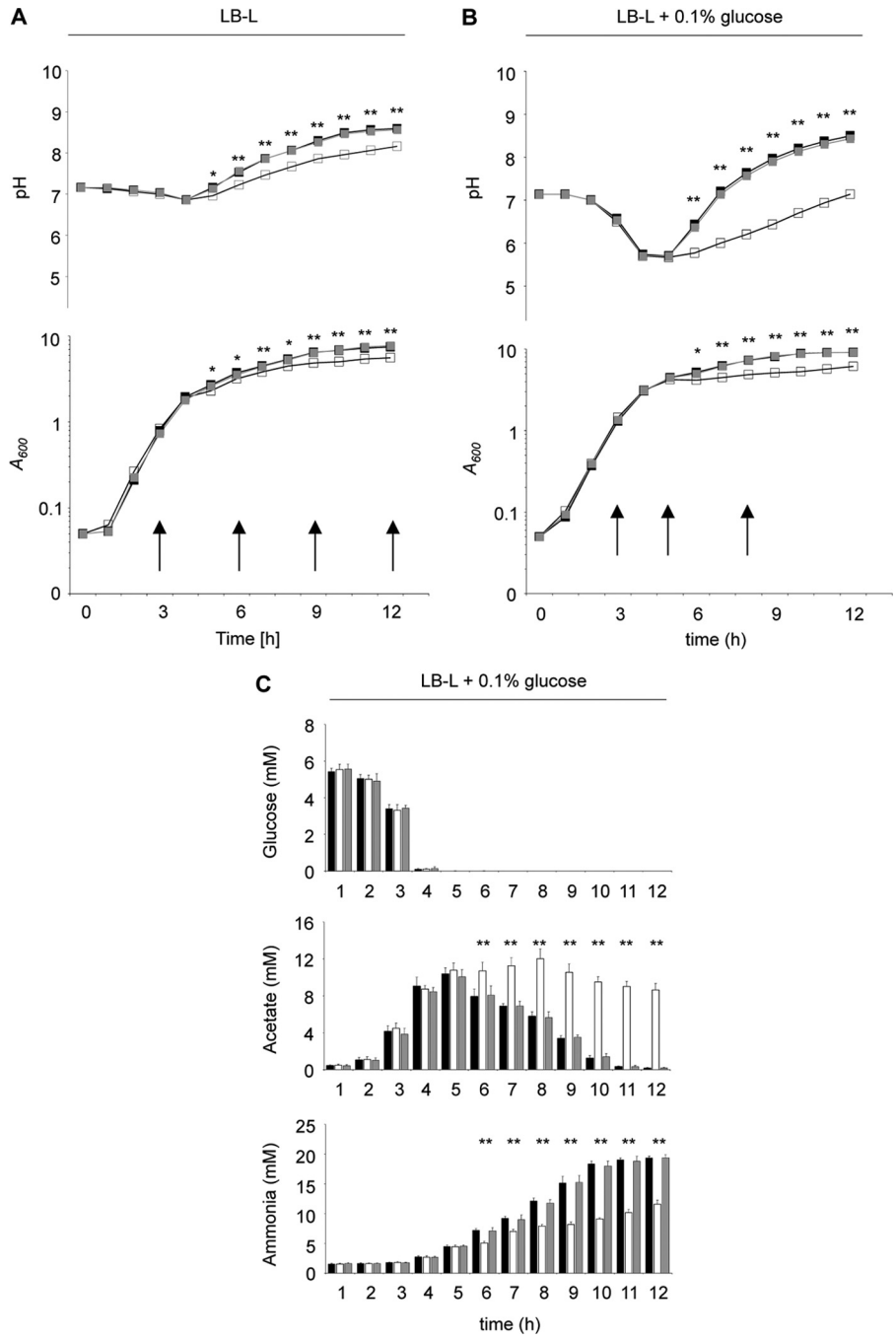

FIGURE 3. **Growth characteristics of *S. aureus* strain Newman (*black symbols*), TH01 (*white symbols*), and TH01c (*gray symbols*).** Culture media pH and A_{600} values during growth in LB-L medium (*A*) and LB-L supplemented with 0.1% glucose (*B*). Time points of sampling for downstream applications (enzyme assays, qRT-PCRs) are indicated by *arrows*. The data presented are mean ± S.D. of at least three independent experiments. Student's *t* test *, $p < 0.05$; **, $p < 0.01$. *C*, glucose, acetate, and ammonia concentrations in the culture supernatants of Newman (*black bars*), TH01 (*white bars*), and TH01c (*gray bars*) cell cultures grown in LB-L + 0.1% glucose. The data presented are mean ± S.D. of at least three independent experiments done in duplicate. Mann-Whitney *U* test. **, $p < 0.01$.

these anti-CcpE Western blots, 33-kDa bands in both the wild-type strain and complemented strain TH01c were observed throughout the growth cycle and, as expected, this band was absent in *ccpE* mutant strain TH01. These data were consistent with the Northern data (Fig. 2*A*) and indicated that CcpE accumulated in the cytosols of the wild-type and TH01c strains during the later stages of growth.

CcpE Affects the in Vitro Growth Yield of S. aureus—To determine whether *ccpE* inactivation affected the physiology of *S. aureus*, we assessed the growth and culture medium pH profiles of strains Newman, TH01, and TH01c in LB-L medium in the absence or presence of 0.1% supplemental glucose (Fig. 3). In LB-L medium lacking glucose, strain TH01 displayed a slight decrease in the growth yield relative to the wild-type and TH01c strains (Fig. 3*A*). Additionally, the pH of the culture medium for strain TH01 was less alkaline than for wild-type and TH01c strains, indicating that the *ccpE* mutant was either impaired in amino acid catabolism or that the accumulation or depletion of organic acids has changed. Supplementation of LB-L with 0.1% glucose increased the overall growth yields of all

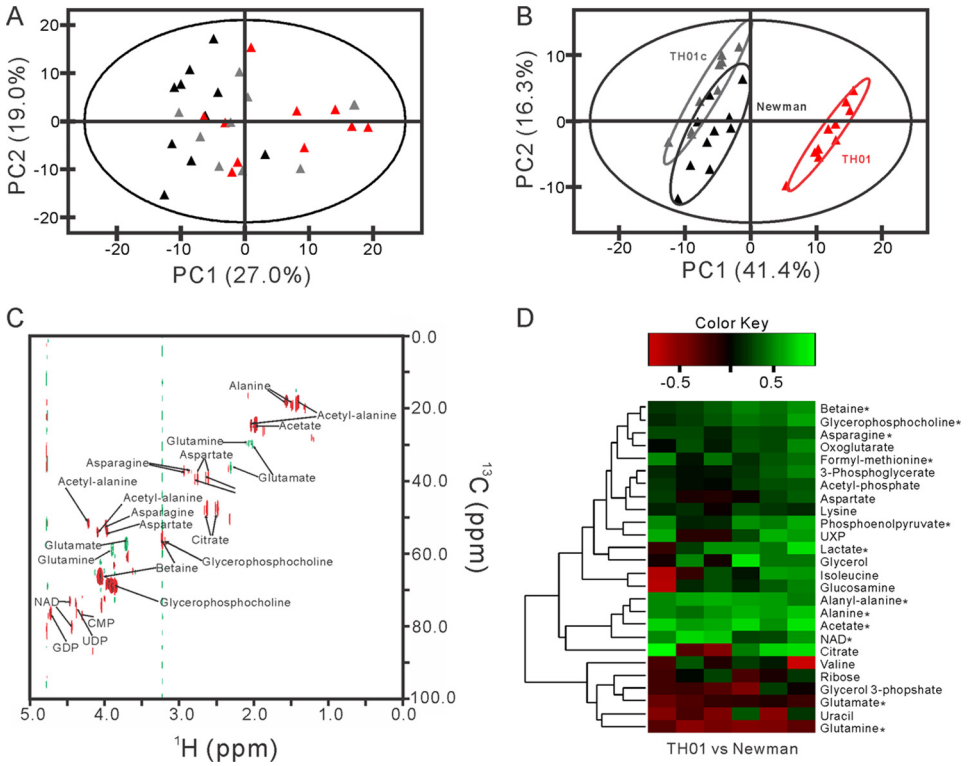

FIGURE 4. **Effect of the *ccpE* deletion on the metabolome of *S. aureus* strain Newman.** *A* and *B*, two-dimensional PCA scores plots generated from the entire one-dimensional ^{1}H NMR spectra of the exponential growth phase (3 h) metabolomes (*A*), and post-exponential growth phase (8 h) metabolomes (*B*) of strains Newman (*black triangles*), TH01 (*red triangles*), and TH01c (*gray triangles*). *C*, two-dimensional ^{1}H,^{13}C-HSQC difference spectrum showing the post-exponential growth phase differences between strains Newman (*green*) and TH01 (*red*). *D*, a heat map of six independent replicates showing the major differences in metabolites produced in post-exponential growth phase by strain TH01 in relationship to strain Newman. Relative concentration changes were plotted as outlined under "Experimental Procedures," using a color-scale from −1 (*red*) to 1 (*green*). The dendrogram depicts hierarchal clustering of the metabolite concentration changes, where metabolites exhibiting the same relative trend and magnitude changes across all replicates are clustered together ($n = 6$). A Student's *t* test was used to determine the statistical significance of each metabolites change between the TH01 and Newman strains (*, $p < 0.05$).

three strains relative to cultures grown in LB-L, but it did not alter the growth rate (Fig. 3*B*). The similarity of the growth rates but the differences in growth yields suggested that the exponential growth phase metabolism was similar but that the post-exponential growth phase metabolism was altered. Consistent with this suggestion, the pH profiles and glucose, acetate, and ammonia accumulation in the medium were nearly identical up until the post-exponential growth phase (Fig. 3). In the post-exponential growth phase, the culture medium of strains Newman and TH01c began to alkalinize as acetate was extracted from the medium for catabolism via the TCA cycle, and ammonia accumulated due to the deamination of amino acids (Fig. 3*C*). In contrast to strains Newman and TH01c, alkalization of the culture medium from strain TH01 was very slow, as both acetate catabolism and ammonia accumulation were repressed. This reduced ability to catabolize acetate and amino acids was also reflected in the decreased biomass generation and final growth yield. As acetate catabolism and amino acid catabolism were repressed, these data suggested that *ccpE* inactivation inhibited/decreased TCA cycle activity.

Deletion of ccpE Alters the S. aureus Metabolome—The deletion of *ccpE* changed the accumulation and depletion of organic acids in the culture medium and the pH profile (Fig. 3), suggesting that *ccpE* inactivation caused significant metabolic changes. To test this hypothesis, strains Newman, TH01, and TH01c were grown in LB-L medium containing 0.1% [^{13}C]glucose and the metabolomes were analyzed by NMR spectroscopy. The metabolomic analysis of strains Newman, TH01, and TH01c grown in LB-L medium containing 0.1% [^{13}C]glucose provided a metabolic snapshot of the exponential (3 h) and post-exponential (8 h) growth phases (Fig. 4). Consistent with growth and pH profiles for the strains (Fig. 3*B*), an exponential growth phase PCA plot (Fig. 4*A*) revealed no significant differences in the metabolomes of strains Newman, TH01, and TH01c. In contrast to the exponential growth phase, *ccpE* inactivation had a major effect on post-exponential growth phase metabolism (Fig. 4, *B–D*, and 5*A*). In particular, carbon flow through the TCA cycle was reduced as evidenced by the accumulation of citrate and the shunting of pyruvate into fermentative pathways. The accumulation of citrate in strain TH01 was also confirmed in bacteria cultivated in LB-L without glucose, using gas chromatography-mass spectrometry (GC-MS) (Fig. 5*B*). The metabolic block in the TCA cycle created by *ccpE* inactivation led to a reduction in the intracellular concentrations of glutamate and glutamine, which affects the availability of nitrogen donors. The decreased ammonia assimilation via glutamate to glutamine may be the cause for an increased concentration of asparagine, which is generated by amination of aspartate via asparaginase. In summary, we can conclude that CcpE is involved in regulating carbon flow through the TCA cycle, independent of glucose or its catabolic products.

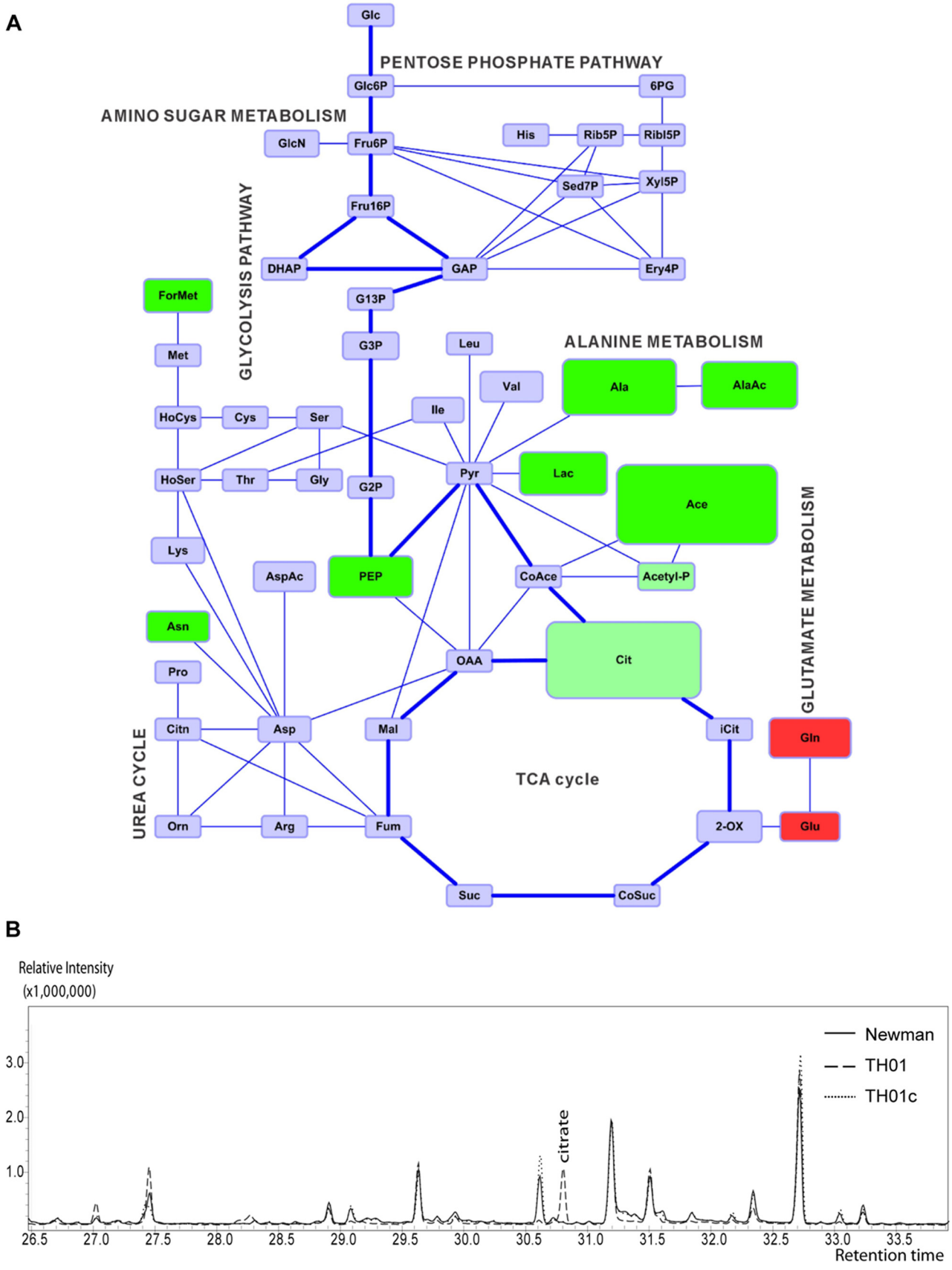

FIGURE 5. **CcpE-dependent changes in the metabolome of *S. aureus*.** *A*, a cytoscape map showing the changes in the central metabolism associated with *ccpE* inactivation. *B*, overlays of representative GC/MS profiles of Newman, TH01, and TH01c whole cell extracts of 8-h LB-L cultures. The elevated citrate peak observed with TH01 is indicated.

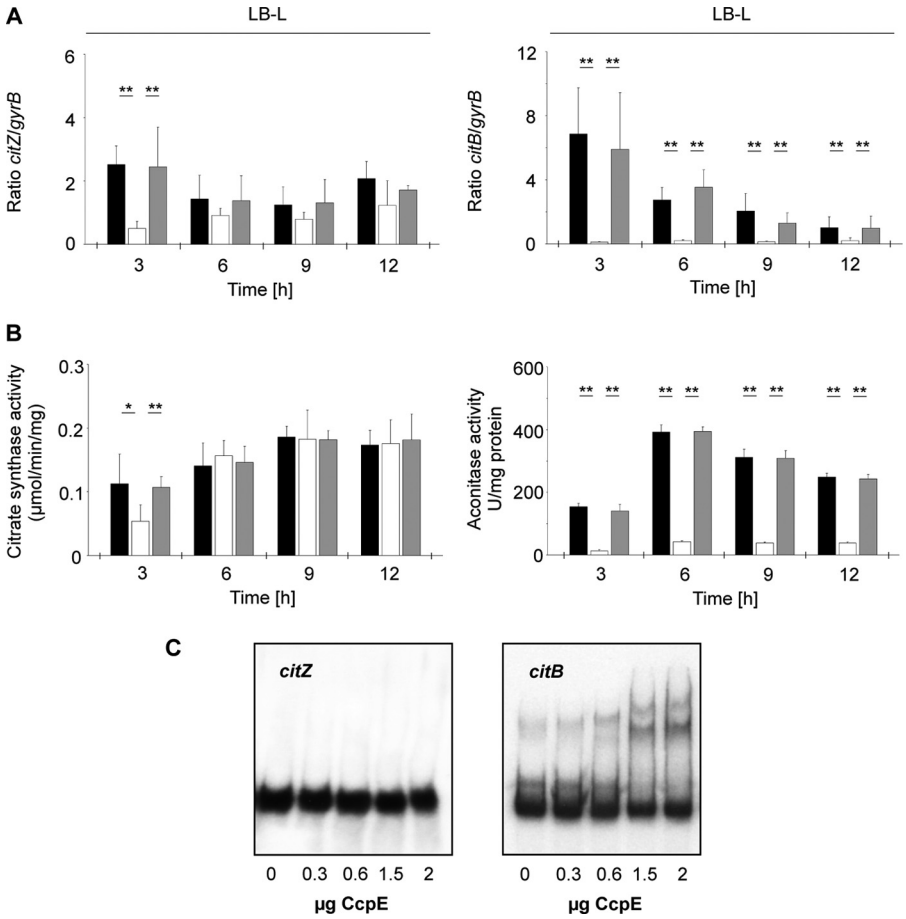

FIGURE 6. **Transcription and activity of *citZ* and *citB* in strain Newman and its derivatives.** *A*, quantitative transcript analysis of *citZ* and *citB* by qRT-PCR of strains Newman (*black bars*), TH01 (*white bars*), and TH01c (*gray bars*) during growth in LB-L. mRNA levels are expressed relative to gyrase B (in numbers of copies per copy of *gyrB*). The data presented are mean ± S.D. of four independent experiments each determined in duplicate. *B*, enzyme activities of citrate synthase, and aconitase of strains Newman (*black bars*), TH01 (*white bars*), and TH01c (*gray bars*) during growth in LB-L. The data are presented as the mean ± S.D. of three independent experiments done in duplicate. Mann-Whitney *U* test *, $p < 0.05$; **, $p < 0.01$. *C*, EMSA using purified CcpE and the DNA probes generated from the *citB* and *citZ* promoters. The PCR-amplified DNA fragments were radioactively labeled and incubated with the amount of purified CcpE indicated. The results are representative of at least two independent experiments.

Inactivation of ccpE Affects Transcription of TCA Cycle Genes and Its Activity—The CcpE encoding ORF in *S. aureus* was identified based on its homology to CcpC in *B. subtilis*. CcpC is involved in the regulation of TCA cycle genes *citZ* and *citB* (5, 6, 8); hence, we hypothesized that CcpE might regulate the same TCA cycle genes in *S. aureus*. To test this assumption, transcription of TCA cycle genes *citZ* and *citB* was assessed by qRT-PCR in strains Newman, TH01, and TH01c grown in LB-L medium (Fig. 6). In the wild-type strain Newman, *citZ* and *citB* mRNAs were at the highest levels just prior to the post-exponential growth phase (Fig. 6*A*). Inactivation of *ccpE* decreased transcription of both *citB* and *citZ*; however, the effect on *citB* was more dramatic. Complementation of the *ccpE* mutation restored *citZ* and *citB* transcription to levels similar to that in the wild-type strain. Thus, to determine whether the differences in *citB* and *citZ* transcription were reflected in enzymatic activity changes, the activities of citrate synthase and aconitase were measured in wild-type, TH01, and TH01c strains as well (Fig. 6*B*). Consistent with the transcriptional data, citrate synthase activity was decreased in strain TH01 at 3 h of growth only, whereas aconitase activity was significantly decreased in TH01 cells in all growth phases. Also consistent with the transcriptional data, complementation of the *ccpE* mutation restored citrate synthase and aconitase enzymatic activities to those in the wild-type strain, strongly suggesting that CcpE is a major positive transcriptional regulator of *citB* in *S. aureus*.

CcpE Binds to the citB Promoter—To assess whether CcpE might directly regulate transcription of *citB* and *citZ* by binding to the respective promoters, we performed EMSAs using the *citZ* and *citB* promoters as probes (Fig. 6*C*). The probe generated from the *citB* promoter shifted with CcpE in a dose-dependent manner; however, the *citZ* promoter region was not shifted by CcpE, suggesting that CcpE directly controls the expression of *citB* but not *citZ*. The similarity of CcpE to CcpC and the fact that citrate accumulated when *ccpE* was inactivated, led us to determine whether citrate would influence CcpE DNA binding activity. In contrast to *B. subtilis* CcpC, the binding activity of CcpE was independent of the concentration of citrate in the binding buffer. Similarly, CcpE binding was independent of NAD^+ and NADH (data not shown). These data suggest that CcpE is not a functional ortholog of CcpC, but a newly described TCA cycle regulator.

CcpE Is Not a Functional Homolog of CcpC—In *B. subtilis*, CcpC regulates transcription of TCA cycle genes in response to

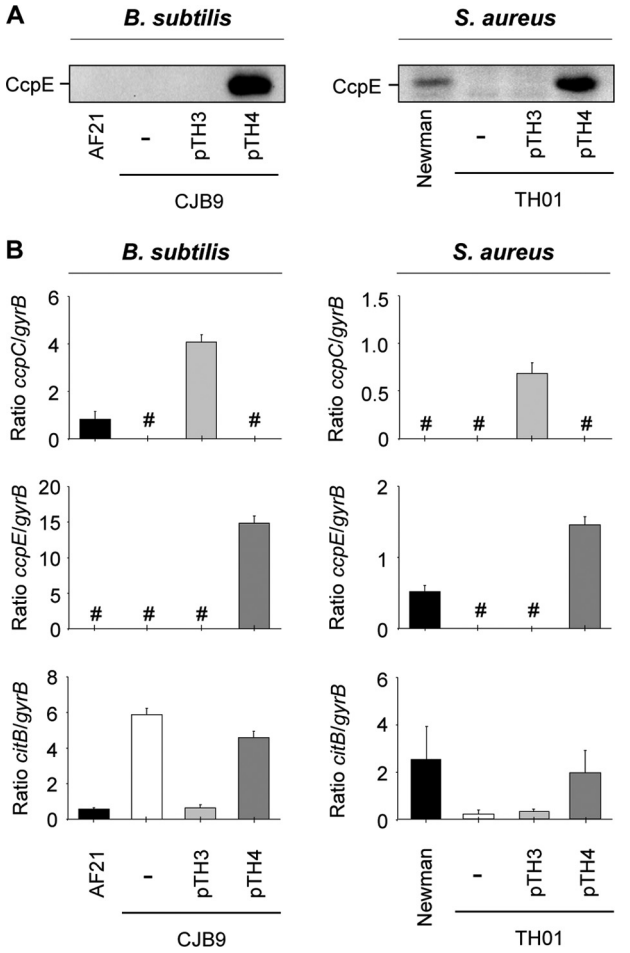

FIGURE 7. **Trans-complementation of *B. subtilis ccpC* and *S. aureus ccpE* mutants.** *A*, Western blot analysis of CcpE in cytosolic extracts of *B. subtilis* strains AF21, CJB9 (AF21::*ccpC*), CJB9 + pTH3 (*ccpC* under the control of its native promoters), CJB9 + pTH4 (ccpC P1/2-*ccpE* fusion), *S. aureus* strains Newman, TH01, TH01 + pTH3, and TH01 + pTH4 after growth in LB-L for 6 h. The results are representative of at least two independent experiments. *B*, quantitative transcript analyses of *ccpC*, *ccpE*, and *citB* by qRT-PCR of *B. subtilis* derivatives grown in TSS minimal medium supplemented with 0.2% (w/v) glutamine and 0.5% (w/v) glucose, and *S. aureus* derivatives grown in LB-L to the mid-exponential growth phase. The data presented are mean ± S.D. of four independent experiments each determined in duplicate. #, transcripts below detection limits.

changes in citric acid, and inactivation of *ccpC* increases the exponential growth phase transcription of *citB* (6). Although *ccpE* inactivation decreased *citB* transcription, its DNA binding properties were not altered by citric acid; out of an abundance of caution, we assessed whether the *S. aureus ccpE* gene could complement a *B. subtilis ccpC* mutant and whether the *B. subtilis ccpC* gene could complement our *S. aureus ccpE* mutant. To do this, plasmids having *ccpC* under the control of its native promoter (pTH3) and a fusion plasmid harboring the *B. subtilis ccpC* P1 and P2 promoters fused to the *S. aureus ccpE* ORF (pTH4) were constructed. These plasmids were transformed into TH01 and the *B. subtilis ccpC* mutant CJB9 (6), respectively, and the final transformants were tested for CcpE by Western blotting and *citB*, *ccpC*, and *ccpE* transcription using qRT-PCR (Fig. 7). As expected, *citB* transcription was increased in *B. subtilis ccpC* mutant strain CJB9 when grown in TSS minimal medium supplemented with 0.2% (w/v) glutamine and 0.5% (w/v) glucose. Complementation of strain CJB9 with *ccpC* under the control of its native promoter, plasmid pTH3, restored *citB* transcription to wild-type levels. In contrast, transforming strain CJB9 with plasmid pTH4, harboring the *S. aureus ccpE* under control of the *B. subtilis ccpC* P1 and P2 promoters, failed to revert *citB* transcription to wild-type levels. To exclude that the inability of CcpE to restore wild-type *citB* mRNA levels was due to a lack of transcription or translation, we assessed *ccpE* transcription using qRT-PCR and CcpE translation by Western blotting. In strain CJB9 containing plasmid pTH4, *ccpE* was strongly transcribed and CcpE was produced in large quantities (Fig. 7*A*), demonstrating that the inability of *ccpE* to complement a *ccpC* mutation was neither due to a failure of transcription nor translation. Similarly, transforming strain TH01 with plasmids pTH3 (containing *ccpC*) or pTH4 (containing *ccpE*) increased *citB* transcription to wild-type levels with *ccpE* but not *ccpC* (Fig. 7*B*). Taken together, these data demonstrate that CcpE is not a functional homolog of CcpC.

DISCUSSION

Central metabolism provides *S. aureus* with 13 biosynthetic intermediates from which it derives all macromolecules; hence, a central metabolism is critically important for growth and survival (44). The TCA cycle is one component of the central metabolism that provides the bacterium with energy, reducing potential, and three of the 13 biosynthetic intermediates. When these 13 biosynthetic intermediates, or the amino acids, nucleic acids, fatty acids, *etc.* that these intermediates produce, are exogenously available, TCA cycle activity is largely repressed (45). In the presence of readily catabolizable carbohydrates, such as glucose, transcription of TCA cycle genes is repressed by CcpA (46). Similarly, transcription of TCA cycle genes is repressed by CodY, a highly conserved Gram-positive repressor that responds to intracellular concentrations of branched-chain amino acids and GTP (reviewed in Ref. 12). When nutrients become growth limiting, transcription of TCA cycle genes is de-repressed and TCA cycle activity dramatically increases, allowing for the utilization of incompletely oxidized organic acids that accumulated in the culture medium (47). This utilization of organic acids through the TCA cycle allows *S. aureus* to generate biosynthetic intermediates needed for precursor and macromolecular synthesis by shunting carbon into gluconeogenesis via P-enolpyruvate. In other words, the TCA cycle is an important metabolic pathway that facilitates *S. aureus* adaption to a nutrient-limited environment. The importance of the TCA cycle to the success of *S. aureus* as a pathogen is illustrated by mutagenesis studies that identified TCA cycle mutants to be attenuated in different mouse models (48, 49) and a *Caenorhabditis elegans*-killing model (50, 51). More recently, the significance of TCA cycle activity during the course of infection was also suggested by a study from Chaffin and colleagues (52), where it was observed that *citB* transcription increased over time in a mouse pneumonia model.

The importance of the TCA cycle in metabolism, survival, and virulence factor synthesis led us to search the *S. aureus* genomic DNA sequence for TCA cycle regulators that are present in *B. subtilis*. One such regulator that is present in *B. subtilis* but undescribed in *S. aureus* is CcpC. We identified a homo-

logue of CcpC in the *S. aureus* genome, which we named CcpE. At the amino acid level, CcpE is similar to the *B. subtilis* CcpC; however, the similarities end there. Deletion of *ccpE* in *S. aureus* dramatically decreased transcription of *citB* and to a lesser extent *citZ*. This decreased transcription resulted in decreased TCA cycle activity, causing a metabolic block in the TCA cycle that increased the intracellular citrate concentration. The increased citrate accumulation and the inability to effectively fully oxidize carbohydrates likely caused the decreased growth yield. These data are in stark contrast to that of CcpC where inactivation of *ccpC* in *B. subtilis* de-represses *citB* and *citZ* transcription (6). Also unlike CcpC, the DNA binding activity of CcpE is not dependent upon the concentration of citrate. In summary, CcpE is a major positive regulator of TCA cycle activity that binds DNA independent of the citrate concentration.

TCA cycle activity has been also associated with virulence in staphylococci. In *S. aureus*, TCA cycle activity was found to be critical for the elaboration of a capsule (53). In contrast, TCA cycle activity negatively affects synthesis of polysaccharide intercellular adhesin and biofilm formation (54). Because CcpE increases TCA cycle activity in *S. aureus*, it is likely that CcpE activity will affect virulence determinant biosynthesis and pathogenesis. Preliminary findings support this hypothesis by indicating that CcpE influences the transcription of a number of virulence factors, and infectivity of *S. aureus* in two independent mouse models. Experiments are ongoing to address this question in greater detail. Another yet unresolved question is which metabolite/co-factors alter the DNA binding properties of CcpE. We know some that do not affect CcpE binding to DNA; namely, citrate and NAD^+/NADH. Last, we are in the process of identifying the DNA binding site for CcpE.

Acknowledgment—We thank A. L. Sonenshein for providing strains AF21 and CJB9 and helpful discussions.

REFERENCES

1. Fujita, Y. (2009) Carbon catabolite control of the metabolic network in *Bacillus subtilis*. *Biosci. Biotechnol. Biochem.* **73,** 245–259
2. Deutscher, J. (2008) The mechanisms of carbon catabolite repression in bacteria. *Curr. Opin. Microbiol.* **11,** 87–93
3. Singh, K. D., Schmalisch, M. H., Stülke, J., and Görke, B. (2008) Carbon catabolite repression in *Bacillus subtilis*. Quantitative analysis of repression exerted by different carbon sources. *J. Bacteriol.* **190,** 7275–7284
4. Lorca, G. L., Chung, Y. J., Barabote, R. D., Weyler, W., Schilling, C. H., and Saier, M. H., Jr. (2005) Catabolite repression and activation in *Bacillus subtilis*. Dependency on CcpA, HPr, and HprK. *J. Bacteriol.* **187,** 7826–7839
5. Kim, H. J., Kim, S. I., Ratnayake-Lecamwasam, M., Tachikawa, K., Sonenshein, A. L., and Strauch, M. (2003) Complex regulation of the *Bacillus subtilis* aconitase gene. *J. Bacteriol.* **185,** 1672–1680
6. Jourlin-Castelli, C., Mani, N., Nakano, M. M., and Sonenshein, A. L. (2000) CcpC, a novel regulator of the LysR family required for glucose repression of the *citB* gene in *Bacillus subtilis*. *J. Mol. Biol.* **295,** 865–878
7. Servant, P., Le Coq, D., and Aymerich, S. (2005) CcpN (YqzB), a novel regulator for CcpA-independent catabolite repression of *Bacillus subtilis* gluconeogenic genes. *Mol. Microbiol.* **55,** 1435–1451
8. Jin, S., and Sonenshein, A. L. (1994) Transcriptional regulation of *Bacillus subtilis* citrate synthase genes. *J. Bacteriol.* **176,** 4680–4690
9. Galinier, A., Haiech, J., Kilhoffer, M. C., Jaquinod, M., Stülke, J., Deutscher, J., and Martin-Verstraete, I. (1997) The *Bacillus subtilis crh* gene encodes a HPr-like protein involved in carbon catabolite repression. *Proc. Natl. Acad. Sci. U.S.A.* **94,** 8439–8444
10. Shivers, R. P., Dineen, S. S., and Sonenshein, A. L. (2006) Positive regulation of *Bacillus subtilis ackA* by CodY and CcpA. Establishing a potential hierarchy in carbon flow. *Mol. Microbiol.* **62,** 811–822
11. Fiegler, H., Bassias, J., Jankovic, I., and Brückner, R. (1999) Identification of a gene in *Staphylococcus xylosus* encoding a novel glucose uptake protein. *J. Bacteriol.* **181,** 4929–4936
12. Somerville, G. A., and Proctor, R. A. (2009) At the crossroads of bacterial metabolism and virulence factor synthesis in *Staphylococci*. *Microbiol. Mol. Biol. Rev.* **73,** 233–248
13. Leibig, M., Krismer, B., Kolb, M., Friede, A., Götz, F., and Bertram, R. (2008) Marker removal in staphylococci via Cre recombinase and different lox sites. *Appl. Environ. Microbiol.* **74,** 1316–1323
14. Rossi, J., Bischoff, M., Wada, A., and Berger-Bächi, B. (2003) MsrR, a putative cell envelope-associated element involved in *Staphylococcus aureus sarA* attenuation. *Antimicrob. Agents Chemother.* **47,** 2558–2564
15. Kennedy, M. C., Emptage, M. H., Dreyer, J. L., and Beinert, H. (1983) The role of iron in the activation-inactivation of aconitase. *J. Biol. Chem.* **258,** 11098–11105
16. Baughn, A. D., and Malamy, M. H. (2002) A mitochondrial-like aconitase in the bacterium *Bacteroides fragilis*. Implications for the evolution of the mitochondrial Krebs cycle. *Proc. Natl. Acad. Sci. U.S.A.* **99,** 4662–4667
17. Bradford, M. M. (1976) A rapid and sensitive method for the quantitation of microgram quantities of protein utilizing the principle of protein-dye binding. *Anal. Biochem.* **72,** 248–254
18. Cheung, A. L., Eberhardt, K. J., and Fischetti, V. A. (1994) A method to isolate RNA from Gram-positive bacteria and mycobacteria. *Anal. Biochem.* **222,** 511–514
19. McCallum, N., Karauzum, H., Getzmann, R., Bischoff, M., Majcherczyk, P., Berger-Bächi, B., and Landmann, R. (2006) *In vivo* survival of teicoplanin-resistant *Staphylococcus aureus* and fitness cost of teicoplanin resistance. *Antimicrob. Agents Chemother.* **50,** 2352–2360
20. Chatterjee, I., Becker, P., Grundmeier, M., Bischoff, M., Somerville, G. A., Peters, G., Sinha, B., Harraghy, N., Proctor, R. A., and Herrmann, M. (2005) *Staphylococcus aureus* ClpC is required for stress resistance, aconitase activity, growth recovery, and death. *J. Bacteriol.* **187,** 4488–4496
21. Valihrach, L., and Demnerova, K. (2012) Impact of normalization method on experimental outcome using RT-qPCR in *Staphylococcus aureus*. *J. Microbiol. Methods* **90,** 214–216
22. Kovács, M., Halfmann, A., Fedtke, I., Heintz, M., Peschel, A., Vollmer, W., Hakenbeck, R., and Brückner, R. (2006) A functional *dlt* operon, encoding proteins required for incorporation of D-alanine in teichoic acids in Gram-positive bacteria, confers resistance to cationic antimicrobial peptides in *Streptococcus pneumoniae*. *J. Bacteriol.* **188,** 5797–5805
23. Schulthess, B., Bloes, D. A., François, P., Girard, M., Schrenzel, J., Bischoff, M., and Berger-Bächi, B. (2011) The σ^B-dependent *yabJ-spoVG* operon is involved in the regulation of extracellular nuclease, lipase, and protease expression in *Staphylococcus aureus*. *J. Bacteriol.* **193,** 4954–4962
24. Halouska, S., Zhang, B., Gaupp, R., Lei, S., Snell, E., Fenton, R. J., Barletta, R. G., Somerville, G. A., and Powers, R. (2013) Revisiting protocols for the NMR analysis of bacterial metabolomes. *J. Integr. OMICS* 10.5584/jiomics.v2013i2013.139
25. Zhang, B., Halouska, S., Schiaffo, C. E., Sadykov, M. R., Somerville, G. A., and Powers, R. (2011) NMR analysis of a stress response metabolic signaling network. *J. Proteome Res.* **10,** 3743–3754
26. Hu, K., Westler, W. M., and Markley, J. L. (2011) Simultaneous quantification and identification of individual chemicals in metabolite mixtures by two-dimensional extrapolated time-zero ^1H-^{13}C HSQC ($HSQC_0$). *J. Am. Chem. Soc.* **133,** 1662–1665
27. Delaglio, F., Grzesiek, S., Vuister, G. W., Zhu, G., Pfeifer, J., and Bax, A. (1995) NMRPipe. A multidimensional spectral processing system based on UNIX pipes. *J. Biomol. NMR* **6,** 277–293
28. Johnson, B. A. (2004) Using NMRView to visualize and analyze the NMR spectra of macromolecules. *Methods Mol. Biol.* **278,** 313–352
29. Wishart, D. S., Knox, C., Guo, A. C., Eisner, R., Young, N., Gautam, B., Hau, D. D., Psychogios, N., Dong, E., Bouatra, S., Mandal, R., Sinelnikov, I., Xia, J., Jia, L., Cruz, J. A., Lim, E., Sobsey, C. A., Shrivastava, S., Huang, P.,

Liu, P., Fang, L., Peng, J., Fradette, R., Cheng, D., Tzur, D., Clements, M., Lewis, A., De Souza, A., Zuniga, A., Dawe, M., Xiong, Y., Clive, D., Greiner, R., Nazyrova, A., Shaykhutdinov, R., Li, L., Vogel, H. J., and Forsythe, I. (2009) HMDB. A knowledge base for the human metabolome. *Nucleic Acids Res.* **37,** D603–D610

30. Cui, Q., Lewis, I. A., Hegeman, A. D., Anderson, M. E., Li, J., Schulte, C. F., Westler, W. M., Eghbalnia, H. R., Sussman, M. R., and Markley, J. L. (2008) Metabolite identification via the Madison Metabolomics Consortium Database. *Nat. Biotechnol.* **26,** 162–164
31. Ulrich, E. L., Akutsu, H., Doreleijers, J. F., Harano, Y., Ioannidis, Y. E., Lin, J., Livny, M., Mading, S., Maziuk, D., Miller, Z., Nakatani, E., Schulte, C. F., Tolmie, D. E., Kent Wenger, R., Yao, H., and Markley, J. L. (2008) BioMagResBank. *Nucleic Acids Res.* **36,** D402-D408
32. Kanehisa, M., Araki, M., Goto, S., Hattori, M., Hirakawa, M., Itoh, M., Katayama, T., Kawashima, S., Okuda, S., Tokimatsu, T., and Yamanishi, Y. (2008) KEGG for linking genomes to life and the environment. *Nucleic Acids Res.* **36,** D480–D484
33. Killcoyne, S., Carter, G. W., Smith, J., and Boyle, J. (2009) Cytoscape. A community-based framework for network modeling. *Methods Mol. Biol.* **563,** 219–239
34. Kanehisa, M., and Goto, S. (2000) KEGG. Kyoto encyclopedia of genes and genomes. *Nucleic Acids Res.* **28,** 27–30
35. Caspi, R., Foerster, H., Fulcher, C. A., Kaipa, P., Krummenacker, M., Latendresse, M., Paley, S., Rhee, S. Y., Shearer, A. G., Tissier, C., Walk, T. C., Zhang, P., and Karp, P. D. (2008) The MetaCyc Database of metabolic pathways and enzymes and the BioCyc collection of Pathway/Genome Databases. *Nucleic Acids Res.* **36,** D623–D631
36. Nguyen, B. D., Meng, X., Donovan, K. J., and Shaka, A. J. (2007) SOGGY, solvent-optimized double gradient spectroscopy for water suppression. A comparison with some existing techniques. *J. Magn. Reson.* **184,** 263–274
37. Halouska, S., and Powers, R. (2006) Negative impact of noise on the principal component analysis of NMR data. *J. Magn. Reson.* **178,** 88–95
38. Worley, B., Halouska, S., and Powers, R. (2013) Utilities for quantifying separation in PCA/PLS-DA scores plots. *Anal. Biochem.* **433,** 102–104
39. Werth, M. T., Halouska, S., Shortridge, M. D., Zhang, B., and Powers, R. (2010) Analysis of metabolomic PCA data using tree diagrams. *Anal. Biochem.* **399,** 58–63
40. Bischoff, M., Dunman, P., Kormanec, J., Macapagal, D., Murphy, E., Mounts, W., Berger-Bächi, B., and Projan, S. (2004) Microarray-based analysis of the *Staphylococcus aureus* σ^B regulon. *J. Bacteriol.* **186,** 4085–4099
41. Deora, R., and Misra, T. K. (1996) Characterization of the primary σ factor of *Staphylococcus aureus*. *J. Biol. Chem.* **271,** 21828–21834
42. Rao, L., Karls, R. K., and Betley, M. J. (1995) *In vitro* transcription of pathogenesis-related genes by purified RNA polymerase from *Staphylococcus aureus*. *J. Bacteriol.* **177,** 2609–2614
43. Maddocks, S. E., and Oyston, P. C. (2008) Structure and function of the LysR-type transcriptional regulator (LTTR) family proteins. *Microbiology* **154,** 3609–3623
44. Somerville, G. A., and Proctor, R. (2009) in *Staphylococci in Human Disease*, (Crossley, K. B., Jefferson, K. K., Archer, G. L., and Fowler, V. G., eds) 2nd Ed., pp. 3–18, Wiley-Blackwell, Oxford, UK
45. Strasters, K. C., and Winkler, K. C. (1963) Carbohydrate metabolism of *Staphylococcus aureus*. *J. Gen. Microbiol.* **33,** 213–229
46. Seidl, K., Müller, S., François, P., Kriebitzsch, C., Schrenzel, J., Engelmann, S., Bischoff, M., and Berger-Bächi, B. (2009) Effect of a glucose impulse on the CcpA regulon in *Staphylococcus aureus*. *BMC Microbiol.* **9,** 95
47. Somerville, G. A., Chaussee, M. S., Morgan, C. I., Fitzgerald, J. R., Dorward, D. W., Reitzer, L. J., and Musser, J. M. (2002) *Staphylococcus aureus* aconitase inactivation unexpectedly inhibits post-exponential-phase growth and enhances stationary-phase survival. *Infect. Immun.* **70,** 6373–6382
48. Coulter, S. N., Schwan, W. R., Ng, E. Y., Langhorne, M. H., Ritchie, H. D., Westbrock-Wadman, S., Hufnagle, W. O., Folger, K. R., Bayer, A. S., and Stover, C. K. (1998) *Staphylococcus aureus* genetic loci impacting growth and survival in multiple infection environments. *Mol. Microbiol.* **30,** 393–404
49. Mei, J. M., Nourbakhsh, F., Ford, C. W., and Holden, D. W. (1997) Identification of *Staphylococcus aureus* virulence genes in a murine model of bacteraemia using signature-tagged mutagenesis. *Mol. Microbiol.* **26,** 399–407
50. Begun, J., Sifri, C. D., Goldman, S., Calderwood, S. B., and Ausubel, F. M. (2005) *Staphylococcus aureus* virulence factors identified by using a high-throughput *Caenorhabditis elegans*-killing model. *Infect. Immun.* **73,** 872–877
51. Bae, T., Banger, A. K., Wallace, A., Glass, E. M., Aslund, F., Schneewind, O., and Missiakas, D. M. (2004) *Staphylococcus aureus* virulence genes identified by bursa aurealis mutagenesis and nematode killing. *Proc. Natl. Acad. Sci. U.S.A.* **101,** 12312–12317
52. Chaffin, D. O., Taylor, D., Skerrett, S. J., and Rubens, C. E. (2012) Changes in the *Staphylococcus aureus* transcriptome during early adaptation to the lung. *PLoS One* **7,** e41329
53. Sadykov, M. R., Mattes, T. A., Luong, T. T., Zhu, Y., Day, S. R., Sifri, C. D., Lee, C. Y., and Somerville, G. A. (2010) Tricarboxylic acid cycle-dependent synthesis of *Staphylococcus aureus* type 5 and 8 capsular polysaccharides. *J. Bacteriol.* **192,** 1459–1462
54. Zhu, Y., Xiong, Y. Q., Sadykov, M. R., Fey, P. D., Lei, M. G., Lee, C. Y., Bayer, A. S., and Somerville, G. A. (2009) Tricarboxylic acid cycle-dependent attenuation of *Staphylococcus aureus in vivo* virulence by selective inhibition of amino acid transport. *Infect. Immun.* **77,** 4256–4264
55. Kreiswirth, B. N., Löfdahl, S., Betley, M. J., O'Reilly, M., Schlievert, P. M., Bergdoll, M. S., and Novick, R. P. (1983) The toxic shock syndrome exotoxin structural gene is not detectably transmitted by a prophage. *Nature* **305,** 709–712
56. Duthie, E. S. (1952) Variation in the antigenic composition of staphylococcal coagulase. *J. Gen. Microbiol.* **7,** 320–326
57. Fouet, A., and Sonenshein, A. L. (1990) A target for carbon source-dependent negative regulation of the *citB* promoter of *Bacillus subtilis*. *J. Bacteriol.* **172,** 835–844
58. Giachino, P., Engelmann, S., and Bischoff, M. (2001) σ^B activity depends on RsbU in *Staphylococcus aureus*. *J. Bacteriol.* **183,** 1843–1852
59. Geisbrecht, B. V., Bouyain, S., and Pop, M. (2006) An optimized system for expression and purification of secreted bacterial proteins. *Protein Expr. Purif.* **46,** 23–32